Supplementary Information for

Identification of source areas of polycyclic aromatic hydrocarbons in Ulsan, South Korea, using hybrid receptor models and the conditional bivariate probability function

Tuyet Nam Thi Nguyen[a,b], Quang Tran Vuong[a], Sang-Jin Lee[a], Hang Xiao[c], Sung-Deuk Choi[a,*]

[a] *Department of Urban and Environmental Engineering, Ulsan National Institute of Science and Technology (UNIST), Ulsan, 44919, Republic of Korea*

[b] *Faculty of Environmental Science, Saigon University, Ho Chi Minh City, 72710, Vietnam*

[c] *Center for Excellence in Regional Atmospheric Environment, Institute of Urban Environment, Chinese Academy of Sciences, Xiamen 361021, China*

Content **Page**

*Corresponding author. Tel: +82 52 217 2811; fax: +82 52 217 2859.
E-mail address: sdchoi@unist.ac.kr (S.-D. Choi).

Text S1. Sampling method, chemical analysis, and QA/QC

Polyurethane foam (PUF) plugs (4.5 cm radius × 5.0 cm height, Ziemer Chromatographie, Germany) and glass fiber filters (GFFs) (20.3 cm × 25.4 cm, Advantec, Japan) were used to collect gaseous and particulate PAHs, respectively. To remove organic contaminants, before deployment, the GFFs were baked at 400 °C for 4 h, and the PUFs were cleaned with acetone and n-hexane for 30 min each, then dried at 60 °C. After the sampling, the GFFs and PUFs were kept in aluminum foil and polyethylene double zippered bags, then stored at −9 °C until analysis.

Prior to extraction, surrogate standards (phenanthrene-d_{10}, chrysene-d_{12}, and perylene-d_{12}) were spiked into the samples. Then, PAHs in the PUFs and GFFs were extracted using Soxhlet extractors for 20 h with 350 mL of hexane/acetone (9:1). The extracts were concentrated using Turbo Vap II (Caliper, USA) and cleaned up on silica gel columns containing 2 g of anhydrous sodium sulfate, 5 g of silica gel (activated at 600 °C for 2 h), and 2 g of anhydrous sodium sulfate. A volume of 70 mL of dichloromethane/hexane (1:3) was used to elute PAHs from the extracts. The samples were further concentrated to 0.5 mL using a nitrogen evaporator (MGS−2200, Eyela, Japan) and spiked with an internal standard (*p*-terphenyl-d_{14}). The final samples were analyzed using a gas chromatograph coupled to a mass spectrometer (GC/MS, 5975C, Agilent, USA). A DB-5MS column (30 m × 0.25 mm × 0.25 μm) was used for analyte separation. The GC temperature program was as follows: 70 °C → 10 °C/min → 240 °C → 5 °C/min → 300 °C.

Blank samples (n = 15) were also added to each extraction batch and treated as the real samples to check contamination during the pre-treatment process. Method detection limits (MDLs) were calculated as described elsewhere[1] and ranged from 0.04 to 0.25 ng/m^3 for the samples. Moreover, the recovery was 53.0–79.4%, 94.5–102%, and 65.0–74.1% for phenanthrene-d_{10}, chrysene-d_{12}, and perylene-d_{12}, respectively.

Table S1. Average number of trajectory endpoints per cell (*s*) used for the calculation of the conventional model ($PSCF^c$), the model adopting the entire trajectory, and the three-dimensional PSCF (3D-PSCF) model, which adopts trajectory endpoints within the mixing or residual layer.

Period	**$PSCF^c$**	**3D-PSCF**
Summer	60	20
Fall	20	10
Winter	10	2
Spring	10	2
All seasons	25	14

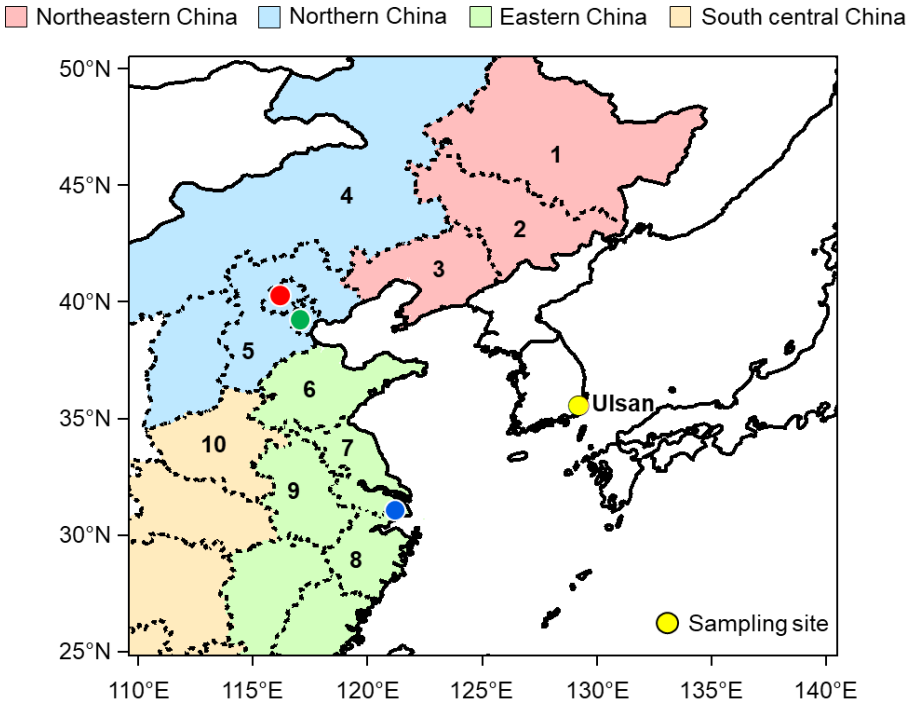

Figure S1. Geographical domain used in this study. The numbers denote provinces in China: (1) Heilongjiang, (2) Jilin, (3) Liaoning, (4) Inner Mongolia, (5) Hebei, (6) Shandong, (7) Jiangsu, (8) Zhejiang, (9) Anhui, and (10) Henan. The red, green, and blue circles represent Beijing, Tianjin, and Shanghai, respectively.

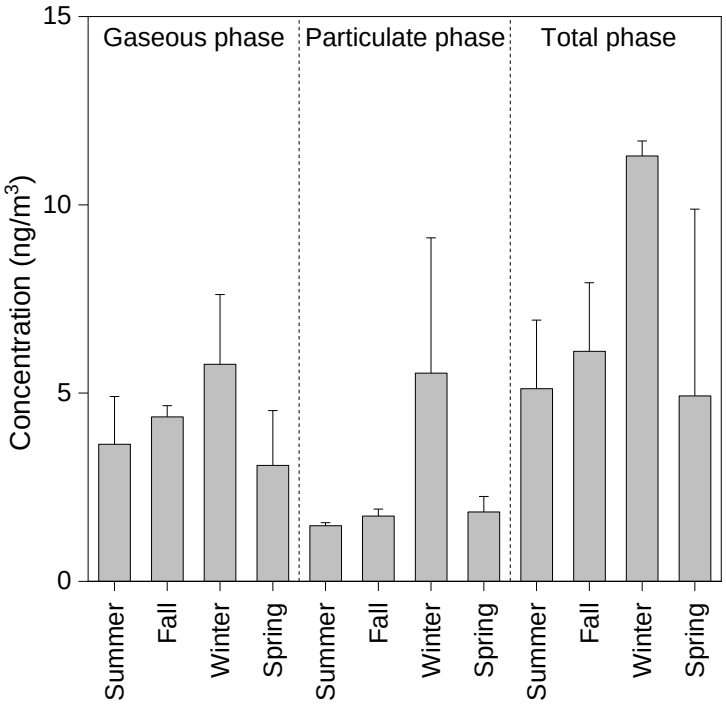

Figure S2. Mean concentrations of gaseous, particulate, and total (gas + particle) Σ_{13} PAHs in the four sampling seasons. The error bars represent standard deviations.

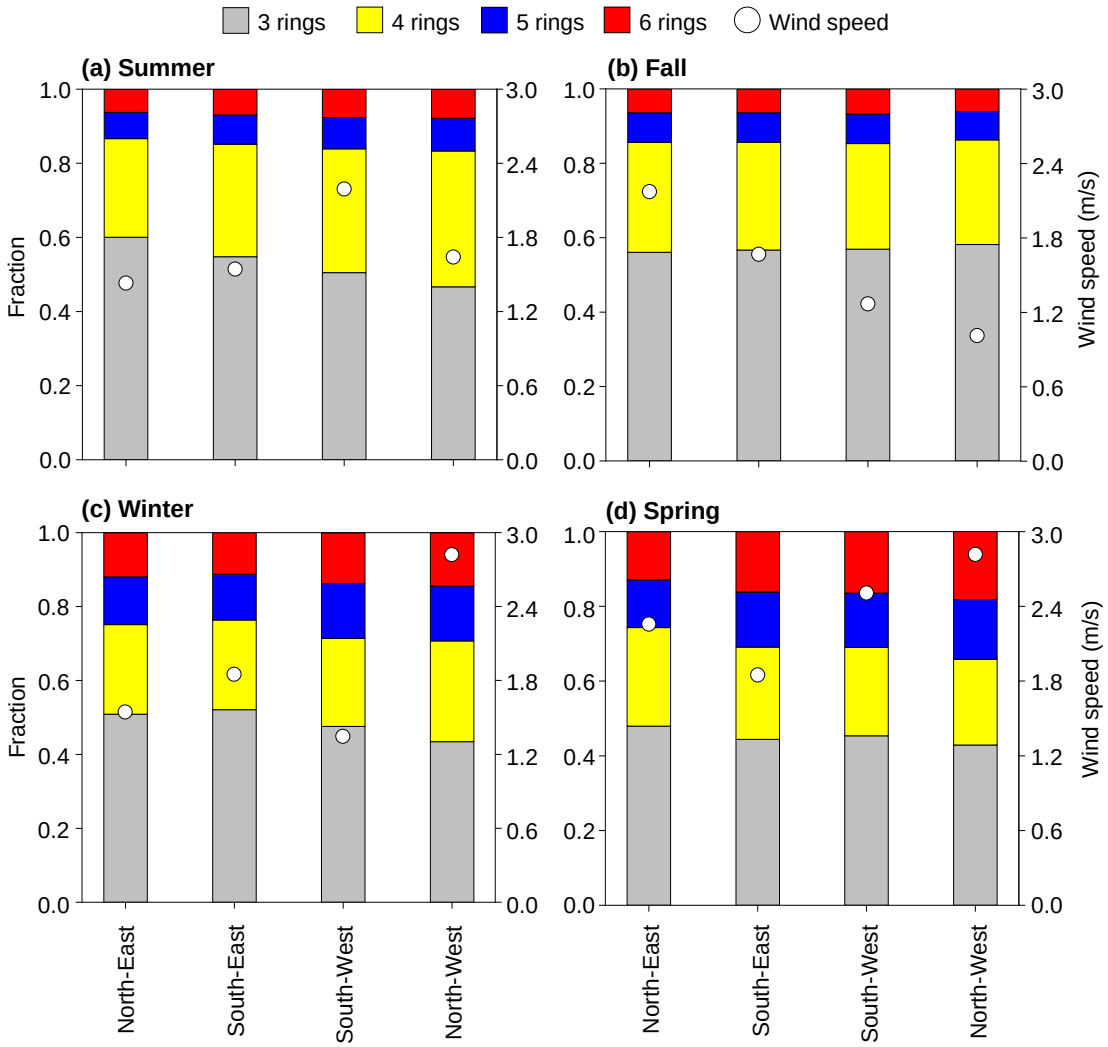

Figure S3. Fractions of total (gaseous + particulate) PAHs by ring numbers associated with wind speed and wind direction: (a) summer, (b) fall, (c) winter, and (d) spring.

Text S2. Concentrations and profiles of PAHs

As shown in Fig. S2, winter showed the highest concentrations of gaseous (mean: 5.77 ng/m^3), particulate (mean: 5.30 ng/m^3), and total (mean: 11.1 ng/m^3) Σ_{13} PAHs. Several parameters could explain this observation, such as increasing combustion for heating and a lower mixing layer height reducing dispersion of air pollutants. Spring showed the second-highest and lowest concentrations for particulate (mean: 1.93 ng/m^3) and gaseous (mean: 3.08 ng/m^3) PAHs, respectively. The reactions of gaseous PAHs with free oxidants (e.g., OH and NO_3)[2] could result in the lowest PAH concentrations in spring. The concentration of PAHs was the lowest in summer (mean: 1.48 ng/m^3), which could be due to an increase of mixing height leading to the greater vertical dispersion of PAHs and the photochemical reactions between particulate

PAHs and O_3.[2] The concentrations of gaseous Σ_{13} PAHs were relatively high in fall (mean: 4.37 ng/m^3) and summer (mean: 3.64 ng/m^3), mainly due to the enhanced evaporation of PAHs with low and medium octanol-air coefficients (e.g., Phe, Flu, and Flt) at high air temperature.

Regarding PAH profiles, the contributions of 5- and 6-ring PAHs (e.g., BaP, BbF, and BghiP) in spring and winter were 1.6−3.0 times higher than those in summer and fall (Fig. S3). These PAHs mainly distribute in the particulate phase. Additionally, the sorption of PAHs to particulate matter (PM) could be enhanced in spring and winter because of the higher PM levels derived from combustion for heating, lower atmospheric temperature, and lower mixing height. Interestingly, the increasing fractions of heavy molecular weight PAHs with 5 and 6 rings were associated with southwesterly and northwesterly winds (Figs. S3a and S3d). These compounds have long atmospheric lifetimes (e.g., 3 to 5 days).[3] Moreover, upwind areas of Ulsan in spring and winter are western South Korea, northern China, and northeastern China; thus, the transport of 5- and 6-ring PAHs emitted from these areas to the receptor site in Ulsan is possible.

In summer and fall, the fractions of 3- and 4-ring PAHs (e.g., Flu, Phe, Flt, and Pyr) increased compared to those in spring and winter because these species have higher volatility and tend to more evaporate from ground surfaces (e.g., soil and surface water) to the atmosphere. In addition, the PAH fractions observed in these seasons were relatively similar regardless of the wind conditions (Figs. S3b and S3c), probably due to the influence of ground or local emission sources.

Text S3. Selection of the optimal weighting function and concentration threshold.

Two weighting functions (W_1 and W_2) and three thresholds (the 50th, 75th, and 90th percentiles of Σ_{13} PAHs) were used to calculate the 3D-PSCF and 3D-CWT models. In general, the weighting functions W_1 and W_2 produced relatively similar PAH source areas. However, the lower values of W_2 slightly reduced the output values of the 3D-PSCF and 3D-CWT models (Fig. S4). Because possible source areas are determined based on higher PSCF and CWT values,[4] these low values of W_2 may lead to inaccurate identification of source areas. Indeed, the 3D-PSCF and 3D-CWT models using W_1 determined that PAHs in Ulsan could be transported from China, especially Shandong, Hebei, Liaoning, and Jilin (Fig. S4a). Nevertheless, these areas were not obviously identified using weighting function W_2 in the

models, especially the 3D-PSCF model (Fig. S4b). Thus, for the reliable identification of source areas, weighting function W_1 was selected for further use in this study.

In terms of the threshold for PSCF calculations, the 3D-PSCF model based on the 90th percentile of Σ_{13} PAHs did not identify northeastern China (e.g., Jilin and Liaoning) as a source area for the PAHs in Ulsan (Fig. S4). These areas, however, were indicated as such using the 3D-PSCF model with 75th and 50th percentiles and the 3D-CWT model (Fig. S4). Therefore, the 90th percentile was considered an unsuitable threshold.

The 3D-PSCF model with the 50th percentile threshold identified potential source areas in Liaoning, Jilin, and the mainland of Japan. However, these areas were not strongly represented by the 3D-PSCF model with the 75th percentile threshold or the 3D-CWT model (Fig. S4), suggesting that they may not be source areas for PAHs in Ulsan. Therefore, the 75th percentile was selected as the optimal threshold for further calculations in this study.

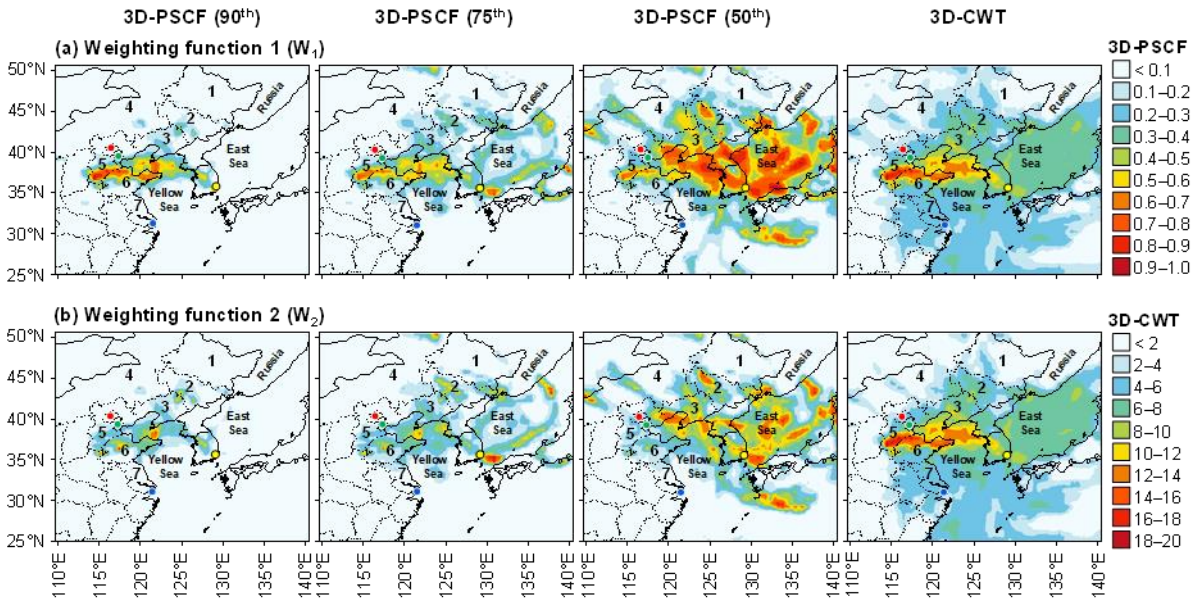

Figure S4. Results for 3D-PSCF with the 90th, 75th, and 50th percentiles for Σ_{13} PAHs and 3D-CWT using two weighting functions: (a) W_1 and (b) W_2. The total (gas + particle) PAH concentrations for the four seasons were used for the calculations.

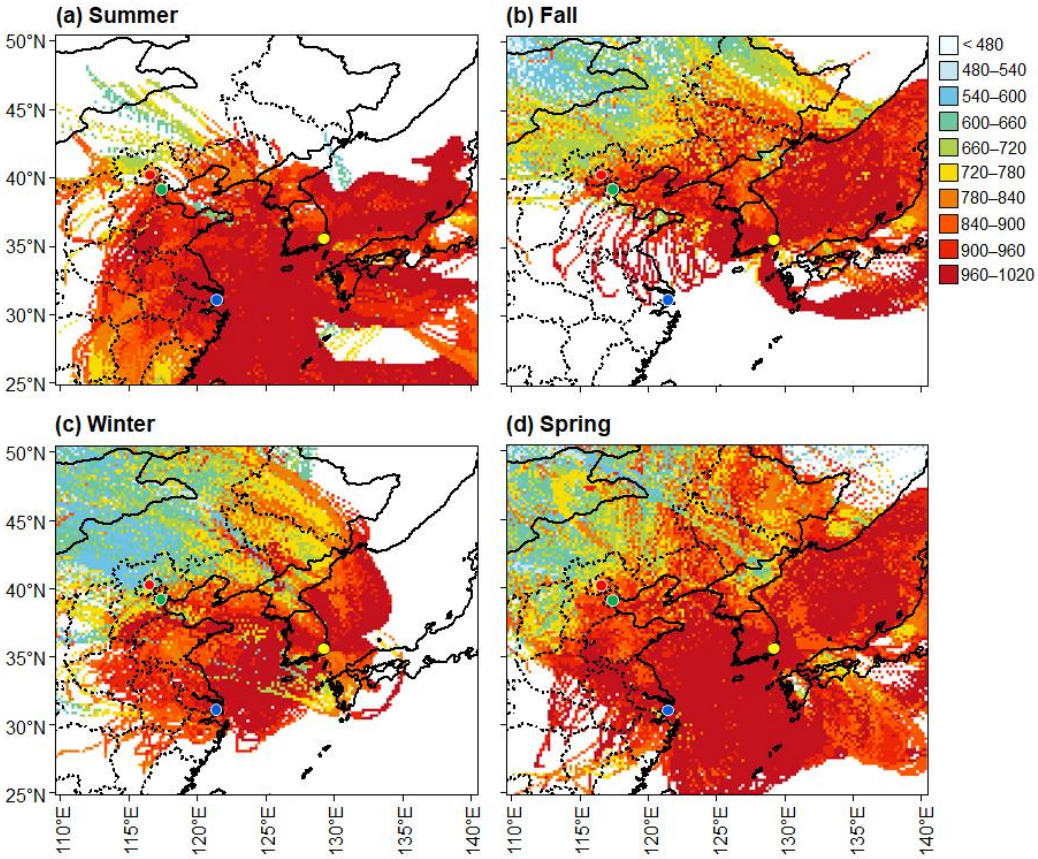

Figure S5. Air pressure (hPa) along the transport routes for backward air trajectories in (a) summer, (b) fall, (c) winter, and (d) spring. Data were simulated using the HYSPLIT model adopting GDAS1 meteorological data.

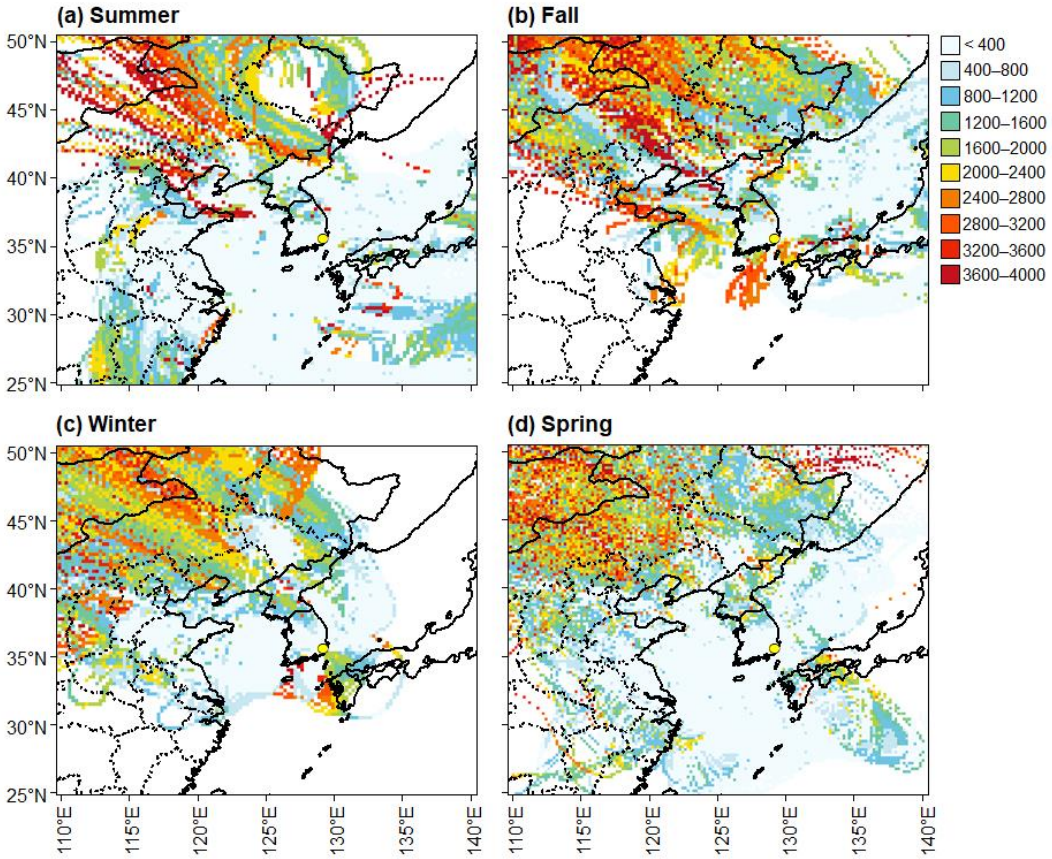

Figure S6. Height (m) of backward air trajectories in (a) summer, (b) fall, (c) winter, and (d) spring. Data were simulated using the HYSPLIT model adopting GDAS1 meteorological data.

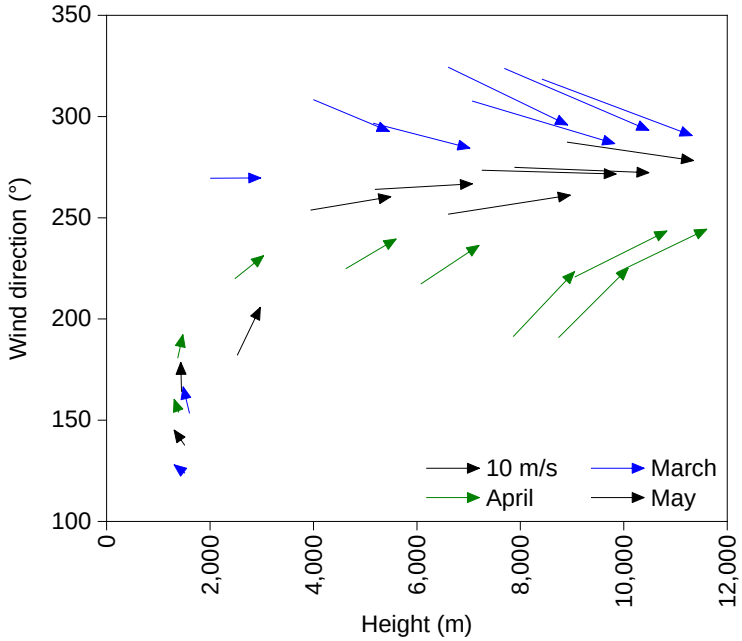

Figure S7. Wind directions at several atmospheric heights at Ulaanbaatar station in Mongolia during spring. The arrows indicate wind directions. Data were obtained from the Department of Atmospheric Science, College of Engineering, University of Wyoming (http://weather.uwyo.edu/upperair/sounding.html).

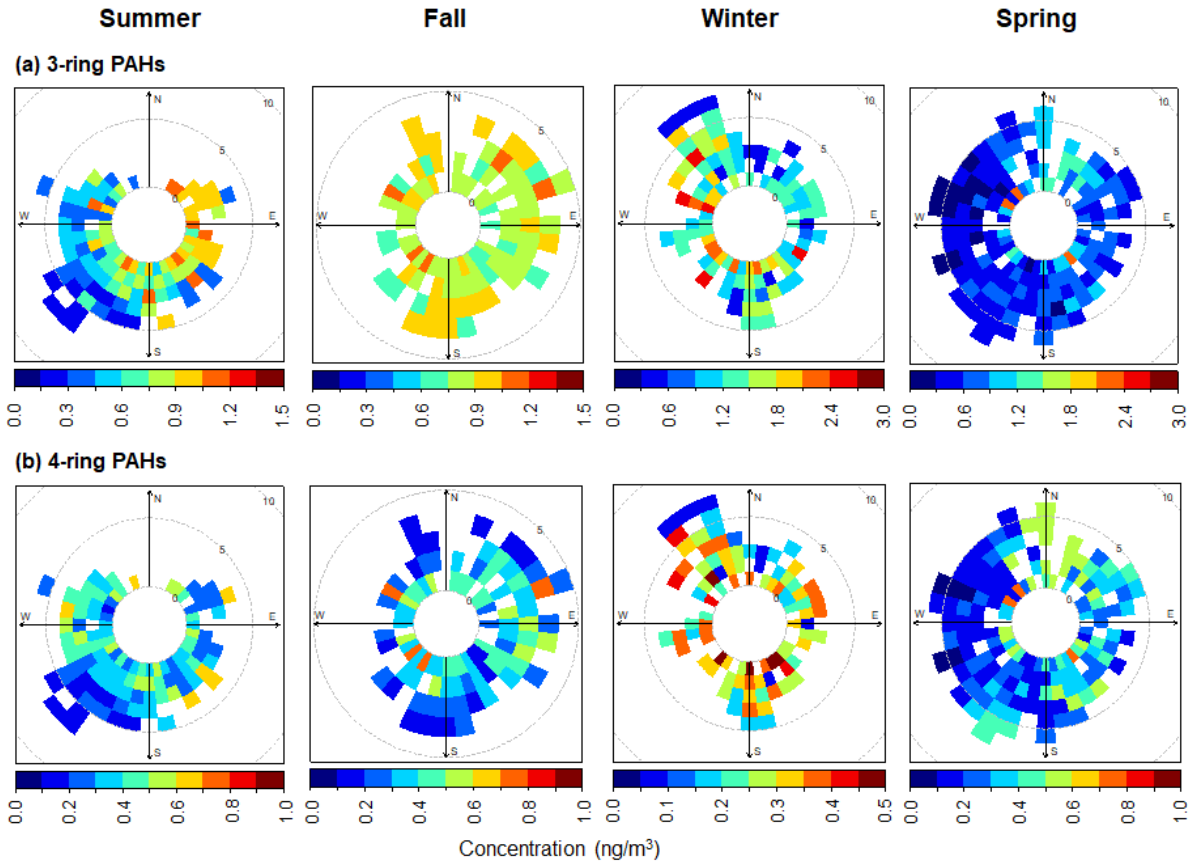

Figure S8. Polar concentration plots for gaseous PAHs shown in (a) 3-ring species and (b) 4-ring species.

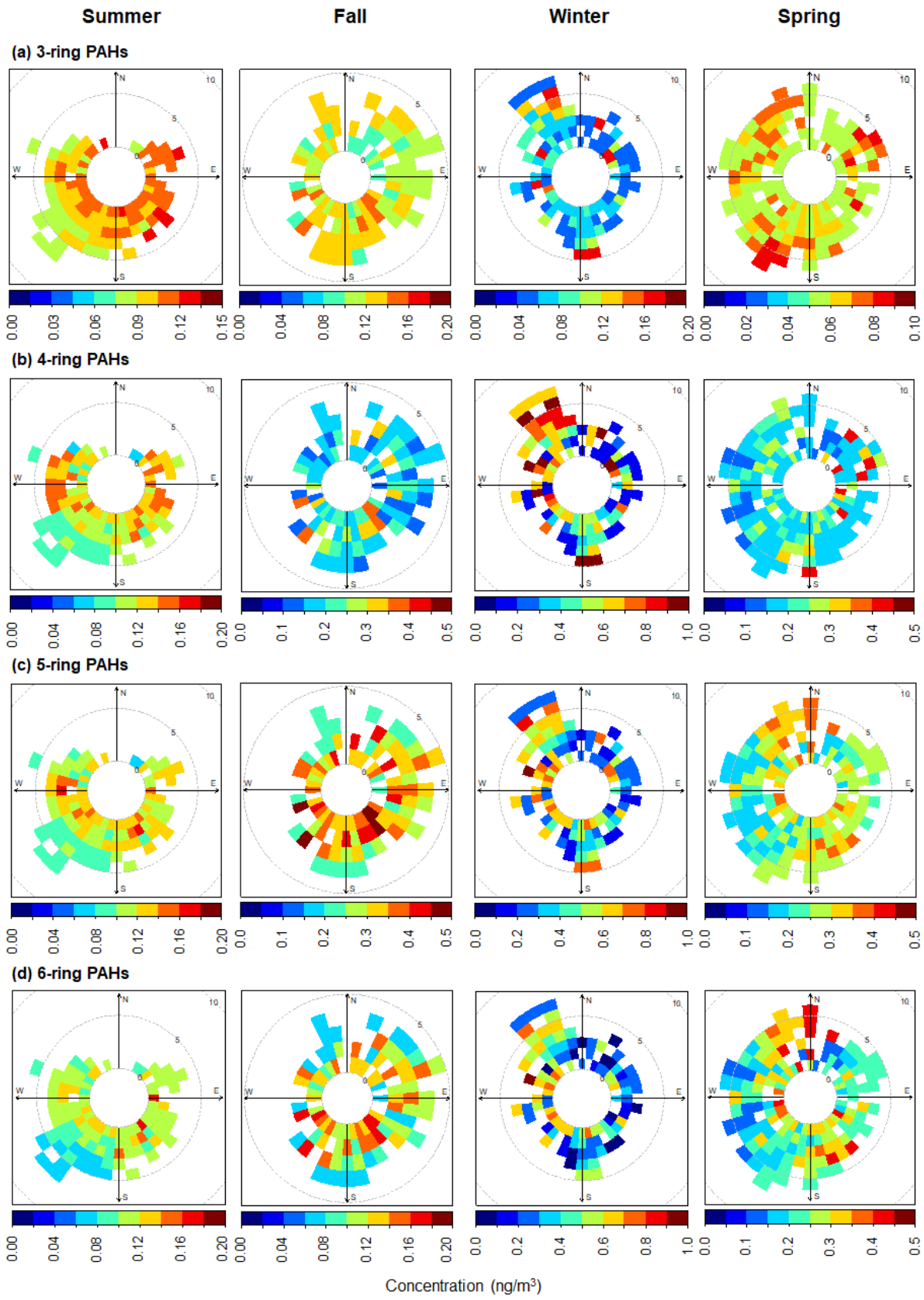

Figure S9. Polar concentration plots for particulate PAHs shown in (a) 3-ring species, (b) 4-ring species, (c) 5-ring species, and (d) 6-ring species.

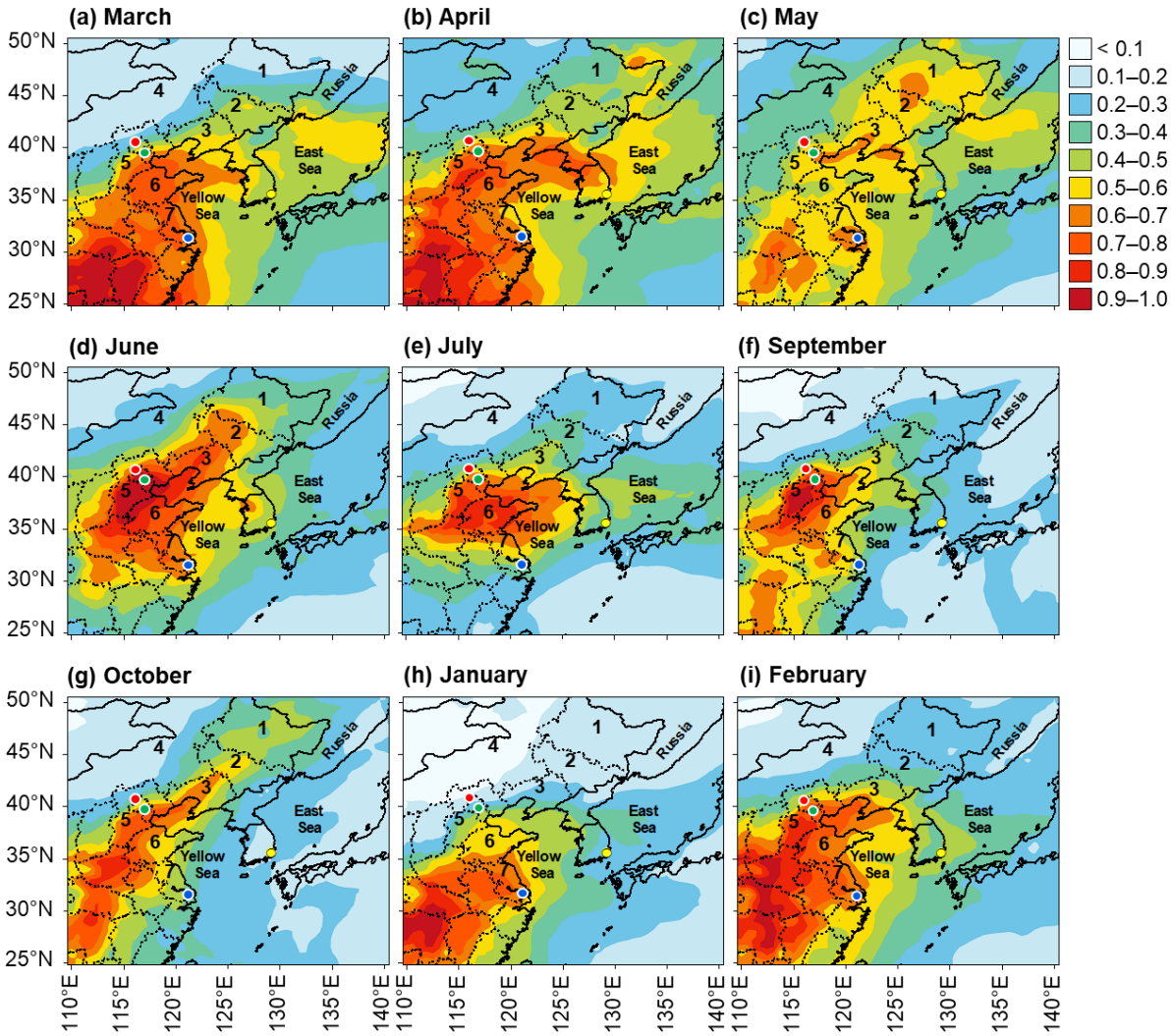

Figure S10. Aerosol optical depth (AOD) observed in Northeast Asia during the study period: (a) March, (b) April, (c) May, (d) June, (e) July, (f) September, (g) October, (h) January, and (i) February. Data were obtained from the Modern-Era Retrospective Analysis for Research and Applications v. 2 (MERRA-2).

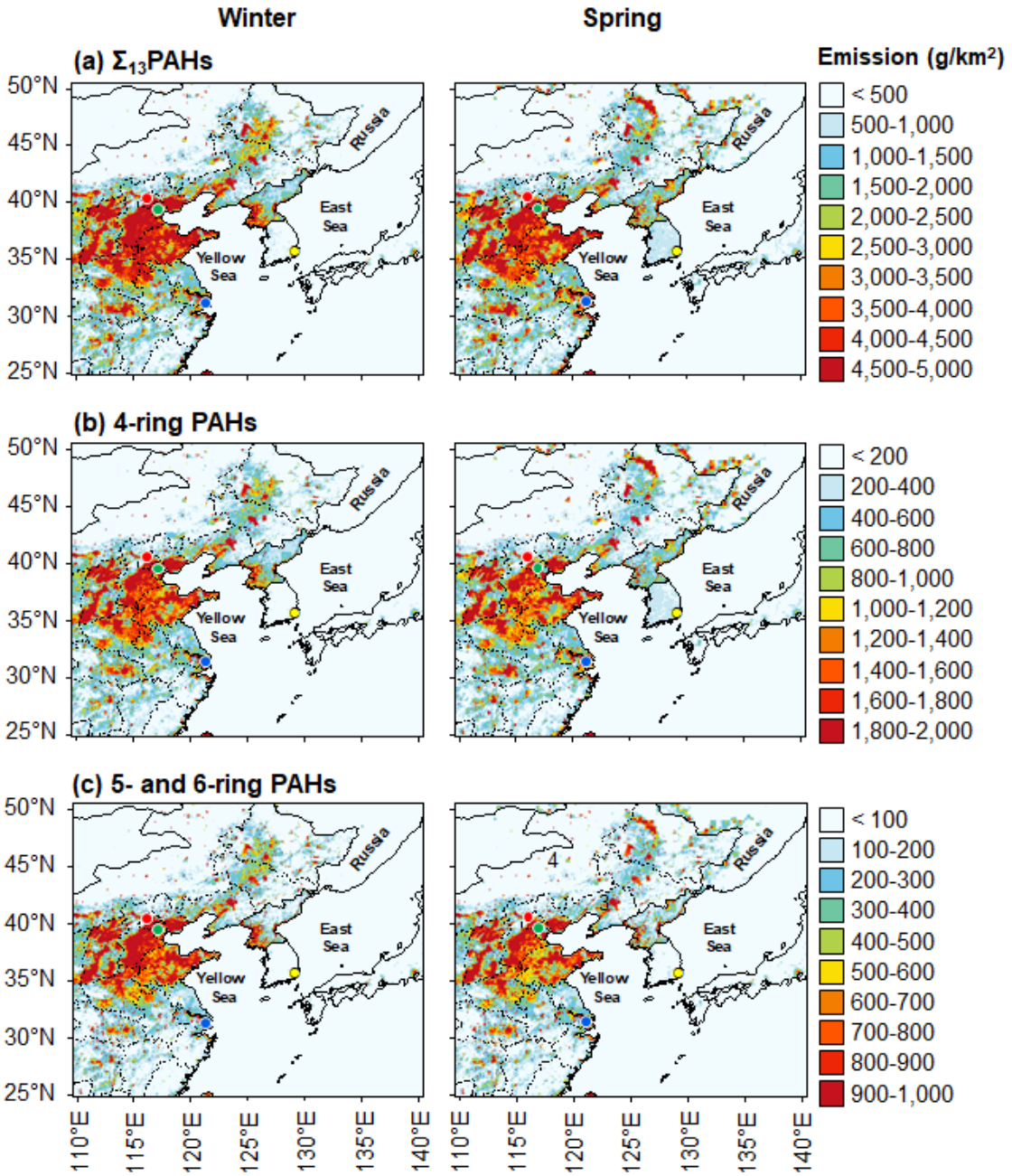

Figure S11. Emission of (a) Σ_{13} PAHs, (b) 4-ring PAHs, and (c) 5- and 6-ring PAHs in Northeast Asia in winter and spring. The red, green, and blue circles represent Beijing, Tianjin, and Shanghai, respectively. Data were obtained from a previous study.[5]

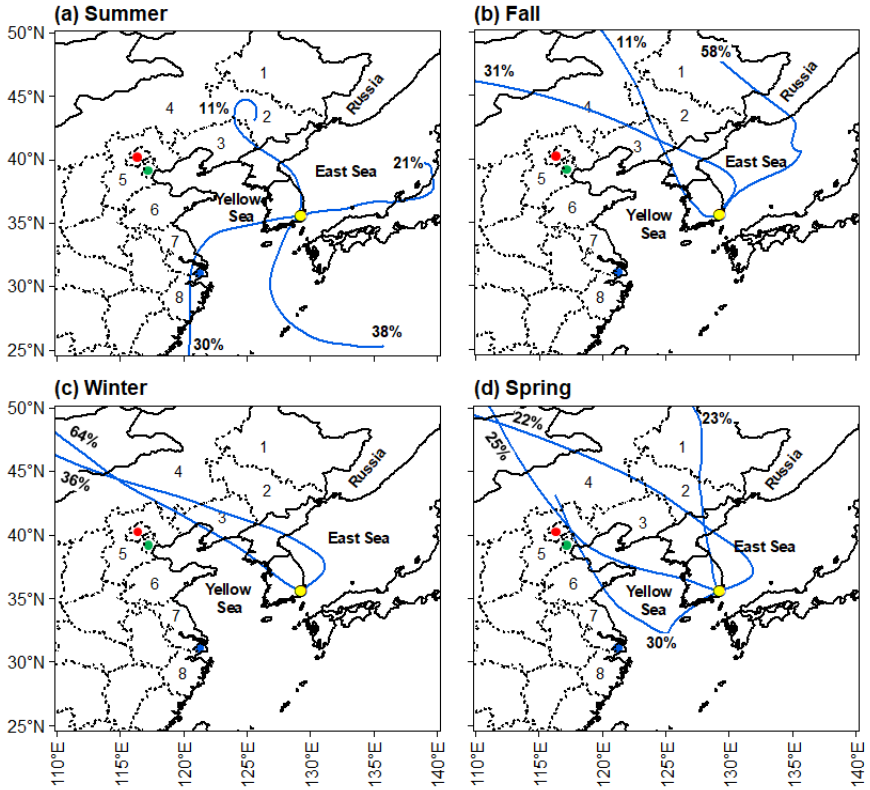

Figure S12. Trajectory cluster analysis in the (a) summer, (b) fall, (c) winter, and (d) spring. The percentages represent the contribution of each cluster.

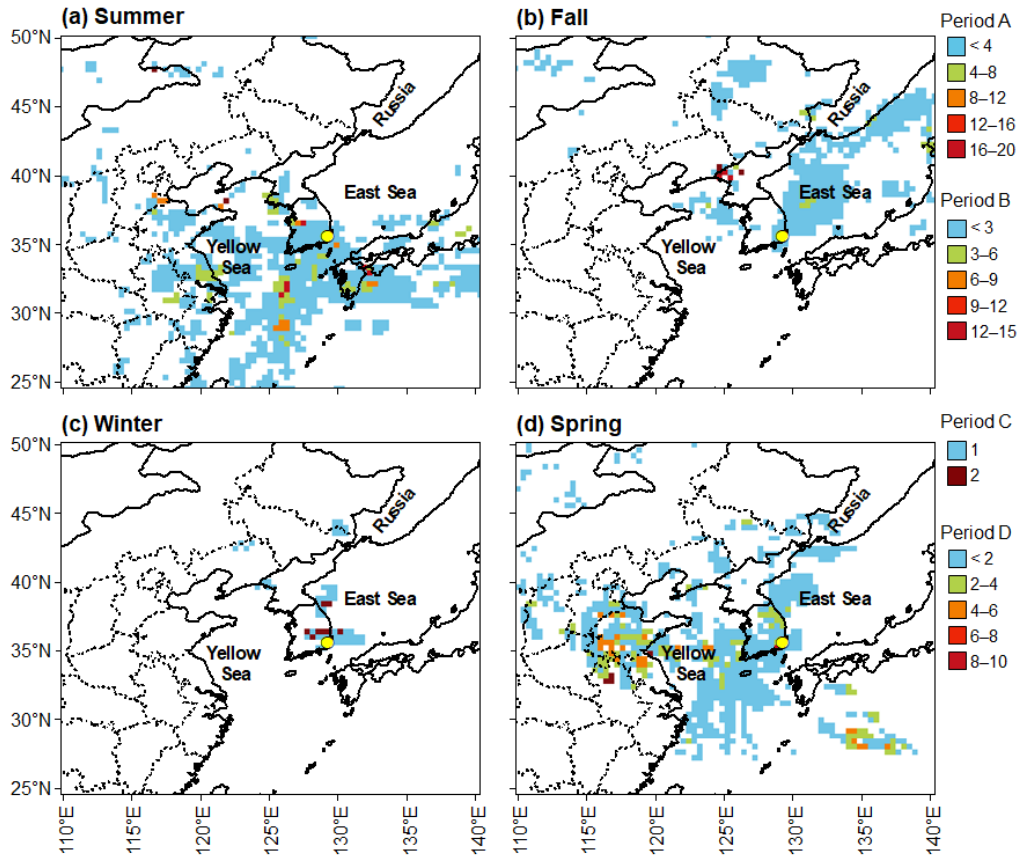

Figure S13. Rainfall levels (mm/h) along the backward air trajectories in (a) summer, (b) spring, (c) winter, and (d) spring. Data were obtained from the HYSPLIT 4 model and GDAS1 meteorological data.

Text S4. References.

1. T. N. T. Nguyen, K.-S. Jung, J. M. Son, H.-O. Kwon and S.-D. Choi, Seasonal variation, phase distribution, and source identification of atmospheric polycyclic aromatic hydrocarbons at a semi-rural site in Ulsan, South Korea, *Environ. Pollut.*, 2018, **236**, 529–539.
2. I. J. Keyte, R. M. Harrison and G. Lammel, Chemical reactivity and long-range transport potential of polycyclic aromatic hydrocarbons – A review, *Chem. Soc. Rev.*, 2013, **42**, 9333–9391.
3. A. N. Neilson, *PAHs and related compounds*, Springer-Verlag Berlin Heidelberg, 1998.
4. P. K. Hopke, N. Gao and M.-D. Cheng, Combining chemical and meteorological data to infer source areas of airborne pollutants, *Chemom. Intell. Lab. Syst.*, 1993, **19**, 187–199.
5. H. Shen, Y. Huang, R. Wang, D. Zhu, W. Li, G. Shen, B. Wang, Y. Zhang, Y. Chen, Y. Lu, H. Chen, T. Li, K. Sun, B. Li, W. Liu, J. Liu and S. Tao, Global atmospheric emissions of polycyclic aromatic hydrocarbons from 1960 to 2008 and future predictions, *Environ. Sci. Technol.*, 2013, **47**, 6415–6424.